

Phenylacetate Catabolism in *Rhodococcus* sp. Strain RHA1: a Central Pathway for Degradation of Aromatic Compounds

Juana María Navarro-Llorens,¹ Marianna A. Patrauchan,² Gordon R. Stewart,² Julian E. Davies,² Lindsay D. Eltis,² and William W. Mohn^{2*}

Departamento de Bioquímica y Biología Molecular I, Universidad Complutense de Madrid, 28040 Madrid, Spain,¹ and Department of Microbiology and Immunology, University of British Columbia, 300-6174 University Blvd., Vancouver, BC V6T 1Z3, Canada²

Received 15 November 2004/Accepted 16 March 2005

In gram-negative bacteria, a pathway for aerobic degradation of phenylacetic acid (PAA) that proceeds via phenylacetyl-coenzyme A (CoA) and hydrolytic ring fission plays a central role in the degradation of a range of aromatic compounds. In contrast, the PAA pathway and its role are not well characterized in gram-positive bacteria. A cluster including 13 *paa* genes encoding enzymes orthologous to those of gram-negative bacteria was identified on the chromosome of *Rhodococcus* sp. strain RHA1. These genes were transcribed during growth on PAA, with 11 of the genes apparently in an operon yielding a single transcript. Quantitative proteomic analyses revealed that at least 146 proteins were more than twice as abundant in PAA-grown cells of RHA1 than in pyruvate-grown cells. Of these proteins, 29 were identified, including 8 encoded by the *paa* genes. Knockout mutagenesis indicated that *paaN*, encoding a putative ring-opening enzyme, was essential for growth on PAA. However, *paaF*, encoding phenylacetyl-CoA ligase, and *paaR*, encoding a putative regulator, were not essential. *paaN* was also essential for growth of RHA1 on phenylacetaldehyde, phenylpyruvate, 4-phenylbutyrate, 2-phenylethanol, 2-phenylethylamine, and L-phenylalanine. In contrast, growth on 3-hydroxyphenylacetate, ethylbenzene, and styrene was unaffected. These results suggest that the range of substrates degraded via the PAA pathway in RHA1 is somewhat limited relative to the range in previously characterized gram-negative bacteria.

Rhodococci are aerobic, gram-positive actinomycetes of high G+C content and are capable of morphological differentiation in response to their environment (e.g., cocci or filaments). These widely occurring organisms are of considerable environmental and biotechnological importance due to their broad metabolic diversity and array of unique enzymatic capabilities. These characteristics are of interest for potential pharmaceutical, environmental, chemical, and energy applications. Rhodococci are well suited for bioremediation due to their capacity for long-term survival in soil, their exceptional ability to degrade hydrophobic pollutants even in the presence of more readily degraded substrates, and their ability to accumulate high levels of heavy metals (11, 20).

Rhodococcus sp. strain RHA1 was originally isolated from gamma-hexachlorocyclohexane-contaminated soil and is one of the best-characterized polychlorinated biphenyl degraders (13). RHA1 uses multiple enzyme systems, including at least three ring-hydroxylating dioxygenases, to degrade biphenyl (9) and has a duplicate set of genes encoding degradation of phthalate (16). A draft assembly of the 9.7-Mb genome (for the current assembly, see <http://www.rhodococcus.ca/>) revealed a large number of genes putatively involved in aromatic-compound degradation, including a cluster of genes described in this report that encodes a phenylacetic acid (PAA) pathway.

PAA arises from the deamination of the aromatic amino acid phenylalanine and is widely distributed in the environ-

ment. An aerobic PAA degradation pathway (Fig. 1) has been described for some gram-negative bacteria, such as *Pseudomonas putida* U and *Escherichia coli* (12). In this pathway, PAA is first transformed to phenylacetyl-coenzyme A (CoA), which subsequently undergoes ring hydroxylation, hydrolytic-ring opening, and further degradation. Until recently, aryl-CoA derivatives were considered to be specific to anaerobic catabolic pathways. As such, the PAA pathway has been proposed to be a hybrid pathway. A similar hybrid pathway responsible for the aerobic degradation of benzoate via benzoyl-CoA was recently described for *Burkholderia xenovorans* LB400 (4, 23). The roles of many catabolic proteins of these pathways remain poorly defined.

In *P. putida* U and *E. coli*, the PAA pathway acts as the key terminal part of the phenylacetyl-CoA catabolon, a complex functional unit that integrates peripheral catabolic pathways and catalyzes the transformation of related compounds via a common metabolite. The phenylacetyl-CoA catabolons of these organisms include a range of compounds, some of them important pollutants, such as styrene and ethylbenzene. This catabolon is also significant for biotechnological applications, such as the enzymatic synthesis of penicillins, the production of intermediates (such as 2-hydroxyphenylacetate or 2-hydroxybenzoate) necessary for the synthesis of many chemical compounds, and the production of bioplastics (12). There is evidence for the existence of the PAA pathway in gram-positive bacteria, including the cloning of putative phenylacetyl-CoA ligase genes from some gram-positive strains (1) and the growth of *Rhodococcus opacus* PD630 on PAA, and evidence that PD630 degrades phenyldecane via PAA (2). However, in contrast to the PAA pathway in gram-negative bacteria, the path-

* Corresponding author. Mailing address: Department of Microbiology and Immunology, University of British Columbia, 300-6174 University Blvd., Vancouver, BC V6T 1Z3, Canada. Phone: (604) 822-4285. Fax: (604) 822-6041. E-mail: wmohn@interchange.ubc.ca.

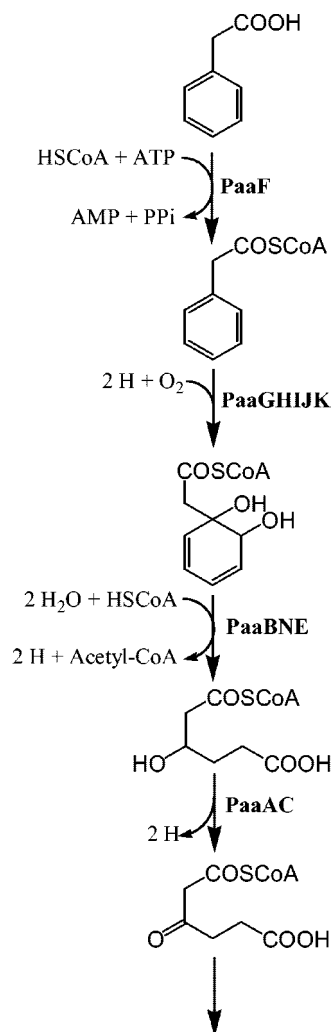


FIG. 1. PAA catabolism pathway (based on that described in reference 8), showing the proposed functions of most *paa* gene products.

way in gram-positive bacteria is not characterized, nor is its role well understood.

In this study, we used proteomic, transcriptional, and gene disruption approaches for the first time to demonstrate a functional PAA pathway and the genes responsible in a gram-positive bacterium. We also determined the pathway's role in the degradation of a range of additional aromatic substrates.

MATERIALS AND METHODS

Bacterial strains, plasmids, and growth conditions. *Rhodococcus* sp. strain RHA1 was kindly provided by M. Fukuda. RHA1 and its mutants were grown with shaking at 200 rpm at 30°C in W minimal salts medium (19) with various organic substrates. Pyruvate and 2-phenylethanol were added directly to the culture medium, and the remaining compounds were added from stock solutions dissolved in NaOH (PAA, 2-hydroxyphenylacetate, 3-hydroxyphenylacetate, and phenylpyruvate) or in water (benzoate, phthalate, mandelate, L-phenylalanine, 4-phenylbutyrate, and tropic acid). Volatile substrates (styrene, ethylbenzene, benzene, phenylacetaldehyde, and biphenyl) were supplied as vapors saturating the culture headspace. For reverse transcriptase PCR (RT-PCR) and proteomic analyses, 500-ml cultures were incubated in 2-liter Erlenmeyer flasks with 20 mM PAA or 20 mM pyruvate. Cells were harvested in mid-exponential growth phase (optical density at 600 nm, 2.0) by centrifugation for 10 min at 4°C and 8,000 ×

g. For proteomic analyses, the cell pellets were flash frozen in liquid nitrogen and stored at -80°C , and subsequent cell manipulation steps were performed at 4°C .

E. coli strains were grown with shaking at 200 rpm at 37°C in Luria-Bertani broth (LB). When appropriate, antibiotics were added at the following concentrations: 50 $\mu\text{g}/\text{ml}$ apramycin (Apr), ampicillin (Amp), kanamycin (Km), or nalidixic acid or 25 $\mu\text{g}/\text{ml}$ chloramphenicol (Cm). *E. coli* WM276/fosmid RF0011cE07 (Cm^r) was provided by the Genome Sciences Centre (Vancouver) and contains a fosmid with a 36.6-kb insert containing the *paa* gene cluster. *E. coli* BW25113/pKD20 and *E. coli* DH10b/pUZ8002 (Km^r) (7) were provided by B. Gust of the John Innes Institute. The plasmid pIJ773 (4.3 kb) (7) was used as the source for a disruption cassette containing the apramycin resistance gene used for PCR-targeted gene replacement. The plasmid pKD20 contains the λ -Red (*gam*, *bet*, *exo*) recombination system (3). The sequences of the PCR primers used in this work are available upon request.

Molecular biology techniques. Plasmid DNA was obtained by rapid alkaline lysis, and DNA manipulations and other molecular biology techniques were done essentially as described previously (18). Genomic DNA extraction was based on a procedure developed for *Listeria monocytogenes* (6). Cell pellets from 3-ml overnight cultures in LB were washed in 1.5 ml of $0.1\times$ SSC ($1\times$ SSC is 0.15 M NaCl plus 0.015 M sodium citrate) and suspended in 300 μl of 0.01 N sodium phosphate buffer in 20% (wt/vol) sucrose (pH 7.0) containing 2.5 mg/ml of lysozyme for an overnight incubation at 37°C . Then, 100 μl of 10% sodium dodecyl sulfate (wt/vol) and 200 μl of Tris-EDTA plus proteinase K at 5 mg/ml were added to the sample and incubated at 37°C for 30 min. Phenol-chloroform extraction, ethanol precipitation, and spooling were performed as described previously (18). RNA was obtained from mid-exponential growth phase cultures by use of RNawiz (Ambion) and by treating the cultures two or three times with DNase (Ambion) until no sign of DNA was detected by PCR. Synthesis of cDNA was done with Superscript III reverse transcriptase (Invitrogen) at 55°C , and the resulting cDNA was treated for 1 h at 37°C with RNase A plus RNase H before being used for RT-PCR. RT-PCRs were carried out in the presence of 4% (vol/vol) dimethyl sulfoxide for 30 cycles (45 s at 94°C , 3 min at 55°C , and 45 s at 72°C) using 0.2 μg cDNA in a 50- μl reaction mixture. Nucleotide and protein sequence similarity searches were done by using the BLASTP, BLASTN, and BLASTX programs from the EMBL server. DNA secondary structure was analyzed using GeneBee (<http://www.genebee.msu.su/>).

Isolation of mutants. The *paaF*, *paaN*, and *paaR* genes were replaced using the λ -Red-based methodology (3) as modified for *Streptomyces* spp. (7) and modified for *Rhodococcus* strain RHA1 (16). Fosmid clones containing the target genes were selected from an RHA1 library (22) and used to transform *E. coli* BW25113 containing the λ -Red recombination plasmid pKD46 (Amp^r). Gene replacement cassettes consisting of Apr^r *oriT* flanked by sequences from both sides of the target gene were amplified by PCR and introduced into *E. coli* BW25113 (pKD46) containing the appropriate fosmid. Successful transformants (containing the Cm^r Apr^r mutagenized fosmid) were verified by PCR. Recombinant fosmids were isolated, introduced into DH10B/pUZ8002, and then transferred to *Rhodococcus* sp. strain RHA1 by intergeneric conjugation. Selection for double recombination was performed with LB plates containing nalidixic acid plus Apr incubated at 30°C for 5 days. The resulting mutant strains had only the target gene deleted with no transcription termination sequence added. These strains were verified by PCR as described above and by Southern blot analysis. Southern blot analysis was performed with 10 μg EcoRI-digested genomic DNA, which was transferred to a nylon membrane and hybridized, in the presence of 50% formamide at 30°C , with digoxigenin-labeled PCR probes amplified from RHA1 (FiF-FiR primers for *paaF*, RiR-RiR for *paaR*, and NiR-NiR for *paaN*).

Proteomic analysis. Cytoplasmic proteins were analyzed by two-dimensional (2D) gel electrophoresis followed by 2D gel quantitative analysis and peptide mass fingerprint analysis essentially as previously described (16). Briefly, cells were thoroughly washed, suspended in a lysis buffer, and disrupted using a bead beater. The cell-free protein extract obtained was either stored at -80°C or used immediately. The first dimension was run using nonlinear IPG strips (Immobiline DryStrips; 24 cm, pH 3 to 7) and 90 μg of protein extract. The IPG strips were then equilibrated and run into 24-by-20-cm gels with 12% sodium dodecyl sulfate-polyacrylamide gel electrophoresis using the ETTAN DALT^{twelve} System (Amersham Biosciences). Protein spots were detected using Sypro Ruby stain, and gels were imaged using a Typhoon 9400 (excitation wavelength, 488 nm; emission wavelength, 610 nm) (Amersham Biosciences). Images were differentially analyzed using Progenesis Workstation software (Nonlinear Dynamics, Durham, NC). The signal intensity of each spot was averaged over gels obtained from three different cultures. Only spots with a minimum normalized volume of 0.002 or greater were further analyzed. For proteins appearing on the gel as a horizontal series of spots, likely due to carbamylation, the pI and molecular weight of only the major spot in the series were recorded, and the

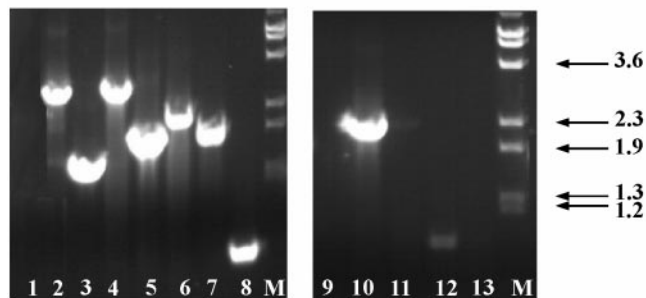
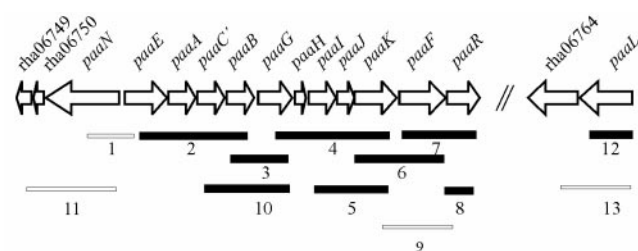


FIG. 2. *paa* gene cluster in *Rhodococcus* sp. strain RHA1 and transcription of the *paa* genes during growth on PAA. Filled bars indicate RT-PCR amplicons detected, and open bars indicate negative RT-PCR assays. Numbers relate gel lanes (bottom) to amplicons (top). RT-PCRs were performed at least three times with different cDNA preparations with consistent results, and a representative experiment is shown. Positive controls with genomic DNA as the template verified all PCRs and the amplicon sizes (not shown). Negative controls without RT verified that DNA did not contaminate any of the RNA templates (not shown). M, size marker of λ DNA, labeled in kilobases, digested with BstEII.

differences in expression were calculated based on the summed signal intensities of all the spots in the series. Protein spots whose intensities increased at least twofold above that of the control (pyruvate-grown cells) were recorded as more abundant. Proteins were identified based on peptide mass fingerprint analyses by use of a Voyager-DE STR matrix-assisted laser desorption ionization-time-of-flight mass spectrometer (Applied Biosystems). Proteins were identified using the Mascot search engine (www.matrixscience.com) and a database generated by in silico digestion of the total RHA1 proteome predicted from the genome assembly as described previously (16).

Analysis of aromatic metabolites. Culture supernatant (40 ml) was passed through a high-capacity C₁₈ Maxi-Clean 300-mg solid-phase extraction cartridge

(Alltech, Deerfield, IL) previously conditioned with methanol and equilibrated with water. The cartridge was rinsed with 2 ml water and then eluted with 2.5 ml methanol. The methanol eluate was evaporated under a stream of nitrogen, and the residue was redissolved in methanol and evaporated again. The residue was taken up in 1 ml of dry methanol. Half of the residue was derivatized with diazomethane, using ethyl acetate (20%) as a cosolvent. Both underivatized and derivatized samples were analyzed by gas chromatography-mass spectroscopy (electron ionization mode) using an Agilent Technologies 6890N network gas chromatograph system equipped with an Agilent 5973 mass selective detector. Compounds were identified by inspection of fragmentation patterns and comparison to the NIST 98 mass spectral library.

RESULTS

***paa* gene cluster in RHA1.** Analysis of the RHA1 draft genome sequence (<http://www.rhodococcus.ca/>) revealed a chromosomal gene cluster encoding a putative PAA biodegradation pathway (Fig. 2). RHA1 was subsequently found to grow on 15 mM PAA as the sole organic substrate. The deduced proteins encoded by the RHA1 *paa* gene cluster (Table 1) as well as the pathway itself (Fig. 1) are similar to those described for *P. putida* U and *E. coli*. Several systems for nomenclature of the *paa* genes have been used, and we have adopted the consensus nomenclature proposed by Luengo et al. (12).

The RHA1 genome also contained paralogs of three *paa* genes, including 1 paralog of *paaC*, 18 of *paaE*, and 9 of *paaF*. The product of open reading frame (ORF) rha07533 shares 42% sequence identity with the 3-hydroxybutyryl-CoA dehydrogenase encoded by *paaC*. ORF rha07533 belongs to a chromosomal cluster of unknown function whose genes were predicted to encode a formamidase, an isocitrate lyase, a methionine synthase, an alcohol dehydrogenase, and a MerR-type transcriptional regulator. The 18 paralogs of the thiolase-encoding *paaE* include *pcaF*, which encodes β -ketoacid succinyl-CoA thiolase (16). Finally, the paralogs of *paaF* share 15 to 28% sequence identity with the phenylacetate-CoA ligase. The ORF with the highest identity, rha10245, is annotated as a putative phenylacetate-CoA ligase-encoding gene. A more detailed annotation of these genes is available at <http://www.rhodococcus.ca/>.

Gene expression analysis by RT-PCR. Most of the *paa* genes appear to lie within a single large operon (Fig. 2). Using Gene-

TABLE 1. ORFs in a chromosomal fragment of RHA1 containing the genes encoding the PAA pathway

Gene (ORF no.)	No. of aa	% GC	EMBL-EBI accession no. (% aa identity); organism	Predicted function
<i>paaL</i> (rha06765)	516	66.2	Q8ENN9 (46.7); <i>Oceanobacillus iheyensis</i>	Na ⁺ -dependent symporter
(rha06764)	425	72.1	Q7WFH4 (45); <i>Bordetella bronchiseptica</i> RB50	Amidase
<i>paaR</i> (rha06762)	342	69.3	P72312 (43.3); <i>Rhodococcus rhodochrous</i>	Nitrilase regulator
<i>paaF</i> (rha06761)	432	66.0	Q82NP4 (70); <i>Streptomyces avermitilis</i>	Aerobic phenylacetate-CoA ligase (EC 6.2.1.30)
<i>paaK</i> (rha06760)	365	67.9	Q93JC1 (71.7); <i>Streptomyces coelicolor</i> A3	Hydroxylating complex V
<i>paaJ</i> (rha06759)	169	67.9	Q93JC2 (69.8); <i>Streptomyces coelicolor</i> A3	Hydroxylating complex IV
<i>paaI</i> (rha06758)	305	68.9	Q93JC3 (54.4); <i>Streptomyces coelicolor</i> A3	Hydroxylating complex III
<i>paaH</i> (rha06757)	101	66.3	Q93JC4 (69.3); <i>Streptomyces coelicolor</i> A3	Hydroxylating complex II
<i>paaG</i> (rha06756)	317	65.5	Q93JC5 (84.5); <i>Streptomyces coelicolor</i> A3	Hydroxylating complex I
<i>paaB</i> (rha06755)	263	73.6	Q9L4S8 (48); <i>Streptomyces collinus</i>	2-Cyclohexenylcarbonyl-CoA isomerase
<i>paaC</i> (rha06754)	284	69.7	Q8FRT3 (61.6); <i>Corynebacterium efficiens</i> YS-314	Putative 3-hydroxybutyryl-CoA dehydrogenase
<i>paaA</i> (rha06753)	257	67.8	Q8FRT4 (64.6); <i>Corynebacterium efficiens</i> YS-314	Putative enoyl-CoA hydratase I
<i>paaE</i> (rha06752)	406	73.4	Q8FRT5 (68.1); <i>Corynebacterium efficiens</i> YS-314	Putative beta-ketoacyl CoA thiolase
<i>paaN</i> (rha06751)	634	69.1	Q92TG5 (68); <i>Rhizobium meliloti</i>	Putative aldehyde dehydrogenase protein (EC 1.2.1.-) ring-opening enzyme
(rha06750)	105	64.5	Q93EX2 (52); <i>Rhodococcus ruber</i>	EthD, from the ethyl <i>tert</i> -butyl ether degradation cluster
(rha06749)	137	69.8	Q93JC6 (65.7); <i>Streptomyces coelicolor</i> A3	Putative PAA degradation protein (thioesterase)

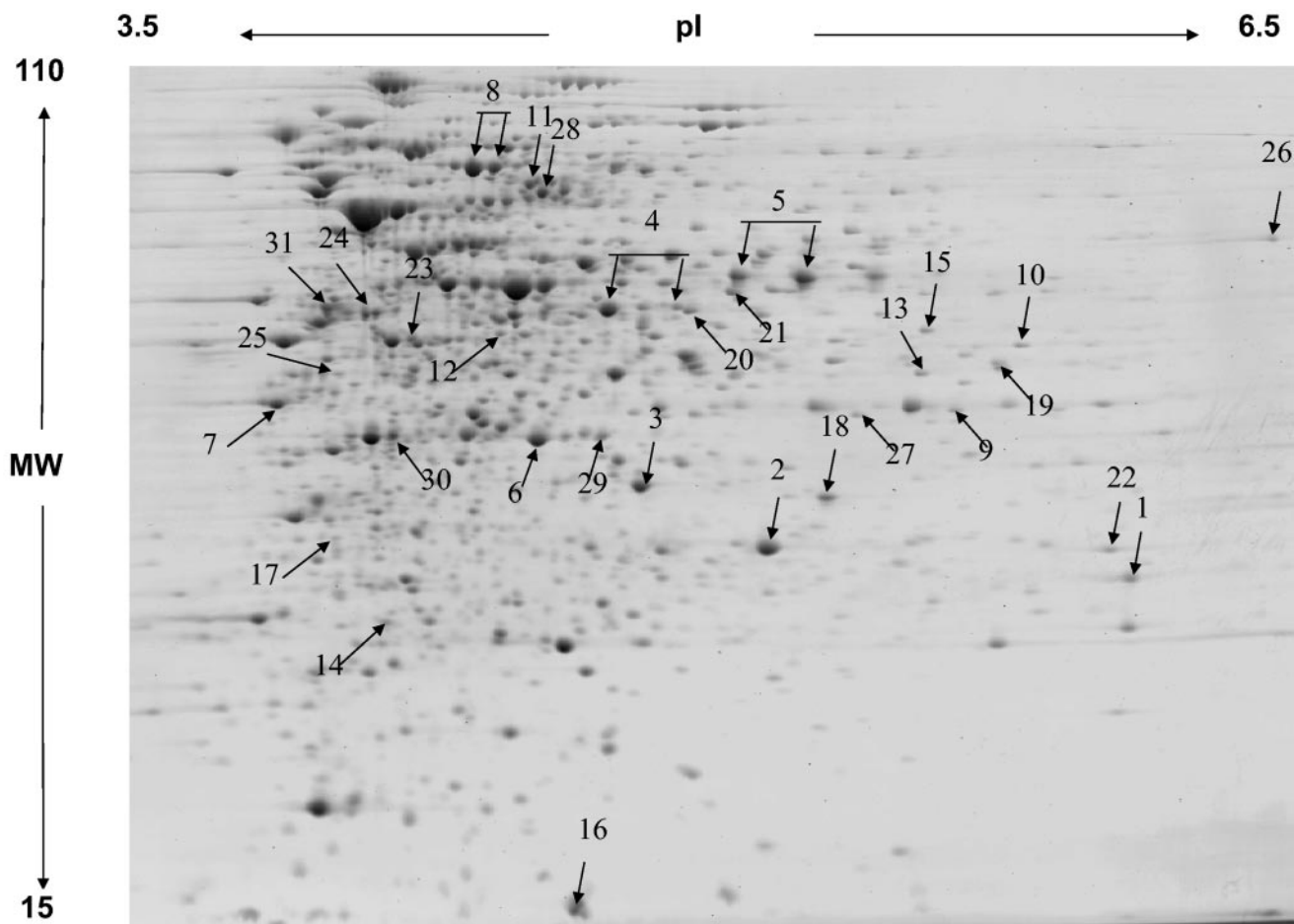


FIG. 3. 2D gel analysis of the proteome of RHA1 grown on PAA. The major proteins associated with phenylacetate catabolism are indicated with arrows. The numbers correspond to spot numbers in Table 2, where the protein names and corresponding ORFs are listed. MW, molecular weight (in thousands).

Bee, we predicted that the secondary structure of the putative polycistronic mRNA from *paaE* to *paaR* would include a weak hairpin (20 bp, -18 kcal/mol) between *paaB* and *paaG* and a strong hairpin downstream of *paaR* (300 bp, -94 kcal/mol). RT-PCR analysis of RHA1 indicates that, in cells grown on PAA, most or all of the *paa* genes are cotranscribed with at least one other *paa* gene (Fig. 2). Two transcripts, including *paaBG* (Fig. 2), indicate that the hairpin between these genes does not terminate all transcripts. We failed to obtain a product spanning *paaKFR* (lane 9), which we cannot explain. However, the product including *paaFR* (lane 7) suggests that *paaR* is cotranscribed with some or all of the other *paa* genes. These results suggest a polycistronic, 9.9-kb transcript including *paaEACBGHIJKFR*. However, smaller transcripts may occur in addition to or instead of the 9.9-kb transcript. The *paaN* and *paaL* genes appear to be individually transcribed, as there was no evidence of cDNA from a *paaL*-*rha06764* transcript and only a very faint band for the *paaN*-*rha06749* transcript.

PAA proteome. A total of approximately 1,430 protein spots were resolved in the proteome of RHA1 grown on PAA (Fig. 3). A quantitative comparison of the proteomes revealed that 75 proteins were at least twofold more abundant during growth on PAA than on pyruvate and that 71 proteins were apparently

unique to the PAA proteome. A total of 29 of the upregulated proteins were identified by mass spectrometric analysis. The calculated and observed pIs and molecular weights of all identified proteins together with the averaged normalized signal intensities observed under each condition are presented in Table S1 (supplemental material available at <http://www.rhodococcus.ca/publications/supplementary/JBact05A.pdf>). Eight of the 13 predicted *paa* gene products (PaaABCEFGIN) were identified (Fig. 3; Table 2). These proteins were detected only in PAA-grown cells, not in pyruvate-grown controls. Of the five predicted Paa proteins that were not found, three have properties that are incompatible with detection by 2D gel electrophoresis, being either too small (PaaH) or too basic (PaaR and PaaL) (Table S1).

In addition to the proteins encoded by the *paa* gene cluster, others encoded by genes elsewhere on the chromosome were associated with growth on PAA. These included the PaaC paralog encoded by *rha07533*, which was not detected in pyruvate-grown cells (Table 2). The *paaC*-encoded protein was more abundant than its paralog. Other proteins that were more abundant in PAA-grown cells included three enzymes involved in the tricarboxylic acid (TCA) cycle: malate dehydrogenase, succinate dehydrogenase, and succinate-CoA ligase. This ob-

TABLE 2. Proteins more abundant in the proteome of RHA1 grown on phenylacetate than in that of RHA1 grown on pyruvate

Protein	ORF no.	Spot no. ^a	No. of peptides matched	Sequence coverage (%)	Normalized signal intensity ^b		Difference (fold) ^c	<i>t</i> -test <i>P</i> value
					Pyruvate	Phenylacetate		
PaaA	rha06753	1	8	45	ND ^d	0.14	70	NA ^e
PaaB	rha06755	2	7	36	ND	0.79	395	NA
PaaC	rha06754	3	8	39	ND	0.61	305	NA
PaaE	rha06752	4	13	51	ND	1.02	510	NA
PaaF	rha06761	5	9	25	ND	0.87	435	NA
PaaG	rha06756	6	5	22	ND	0.43	215	NA
PaaI	rha06758	7	7	35	ND	0.61	305	NA
PaaN	rha06751	8	22	45	ND	1.6	800	NA
3-Hydroxybutyryl-CoA dehydrogenase ^f	rha07533	9	10	36	ND	0.059	30	NA
Acyl-CoA dehydrogenase	rha06610	12	8	30	0.027	0.094	4	0.003553
Malate dehydrogenase	rha08393	24	8	32	0.055	0.33	6	0.000109
Succinate dehydrogenase flavoprotein subunit	rha02921	28	11	23	0.17	0.47	3	0.001381
Succinate-CoA ligase alpha subunit	rha08148	29	9	38	0.017	0.16	9	0.000713

^a Spot numbers correspond to those in Fig. 3.

^b Spot signal intensities were normalized and averaged over three replicate gels (each from a different culture).

^c Difference was calculated as a ratio of averaged normalized signal intensities. For spots that were not detected under one of the conditions, a value of 0.002 was used as the normalized signal intensity (see Materials and Methods). Standard errors are 15%.

^d ND, not detected.

^e NA, not applicable, because the protein spot was not detectable in the pyruvate control proteome.

^f Shares 42% sequence identity with PaaC.

ervation is consistent with the proposed pathway for phenylacetate degradation, the last step of which generates two intermediates of the TCA cycle: acetyl-CoA and succinyl-CoA. We have previously observed (16) that in RHA1 the glyoxylate shunt is upregulated on pyruvate, which supplies only acetyl-CoA to the TCA cycle. This observation is consistent with the relatively higher expression of TCA cycle enzymes on PAA than on pyruvate.

Analysis of knockout mutants. Three genes were selected as targets for knockout mutagenesis in order to confirm their predicted roles in PAA degradation (Fig. 1). Disruption of *paaN* (RHA1_001) completely prevented growth on PAA in liquid medium but had no significant effect on growth on pyruvate or in rich medium (LB). In contrast, the *paaF* mutant (RHA1_002) and the *paaR* mutant (RHA1_003) were able to grow on PAA. However, RHA1_002 grew with a longer lag phase than did the wild type (WT) or RHA1_003 when inoculated from cultures grown in a different substrate (e.g., LB medium). The doubling times on PAA of both RHA1_002 (5.7 ± 0.1 h) and RHA1_003 (5.9 ± 0.1 h) were slightly greater than that of the WT (5.3 ± 0.2 h).

The RHA1 WT and mutants were tested for growth on various additional aromatic substrates to determine which are degraded via the PAA pathway. The RHA1 WT grew on 14 aromatic substrates tested (Table 3) but failed to grow on 2-hydroxyphenylacetate (0.1 to 100 mM) or tropic acid (6 to 30 mM) on either agar plates or liquid medium. The *paaN* mutant was unable to grow on six compounds in addition to PAA. Of those six compounds, the *paaF* mutant was unable to grow on one and impaired in growth on two. The *paaR* mutant was able to grow on the same 14 compounds as the WT at similar rates and to similar final optical densities.

Analysis of metabolites. When the *paaN* mutant (RHA1_001), which is unable to grow on PAA as a sole organic substrate, was grown on 20 mM pyruvate plus 0.15 mM PAA, a yellow color was observed in the medium after 2 days. The yellow color was not observed if RHA1_001 was grown without PAA or if the WT was grown on pyruvate plus PAA. The me-

dium of RHA1_001 grown on pyruvate plus PAA was found to contain tropone ($m/z = 106, 78, 51$), 2-coumaranone ($m/z = 134, 106, 78, 51$), and, after derivatization, the methyl ester of 2-methoxyphenylacetate ($m/z = 180, 121, 91$), in addition to a large amount of undegraded PAA. The medium of the WT had only traces of 2-coumaranone and tropone and had no remaining PAA. Both tropone and 2-coumaranone are yellow and likely contribute to the color observed. After the *paaF* mutant (RHA1_002) was grown on pyruvate with PAA for 2 days, the medium contained undegraded PAA but no other metabolites, confirming a partial defect of this strain in PAA degradation.

DISCUSSION

This study provided conclusive evidence that the *paa* genes of RHA1 encode a functional PAA degradation pathway. First,

TABLE 3. Growth of *Rhodococcus* sp. strain RHA1 and three mutant strains on different substrates^a

Growth substrate (concn) ^b	Growth of ^c :			
	WT RHA1	RHA1_001 (<i>paaN</i>)	RHA1_002 (<i>paaF</i>)	RHA1_003 (<i>paaR</i>)
PAA (15 mM)	+	–	+	+
Styrene (v)	+	+	+	+
Ethylbenzene (v)	+	+	+	+
Benzene (v)	+	+	+	+
Phenylacetaldehyde (v)	+	–	(+)	+
Biphenyl (v)	+	+	+	+
Mandelate (130 mM)	+	+	+	+
Benzoate (20 mM)	+	+	+	+
Phthalate (20 mM)	+	+	+	+
3-Hydroxyphenylacetate (20 mM)	+	+	+	+
4-Phenylbutyrate (30 mM)	+	–	+	+
Phenylpyruvate (20 mM)	+	–	+	+
L-Phenylalanine (12 mM)	+	–	+	+
2-Phenylethylamine (3 mM)	+	–	–	+
2-Phenylethanol (6.2 mM)	+	–	(+)	+

^a All tests were repeated three times.

^b v, volatile compounds added as vapors, according to Materials and Methods;

^c +, growth; –, no growth; (+), poor growth (only isolated colonies grew from streak).

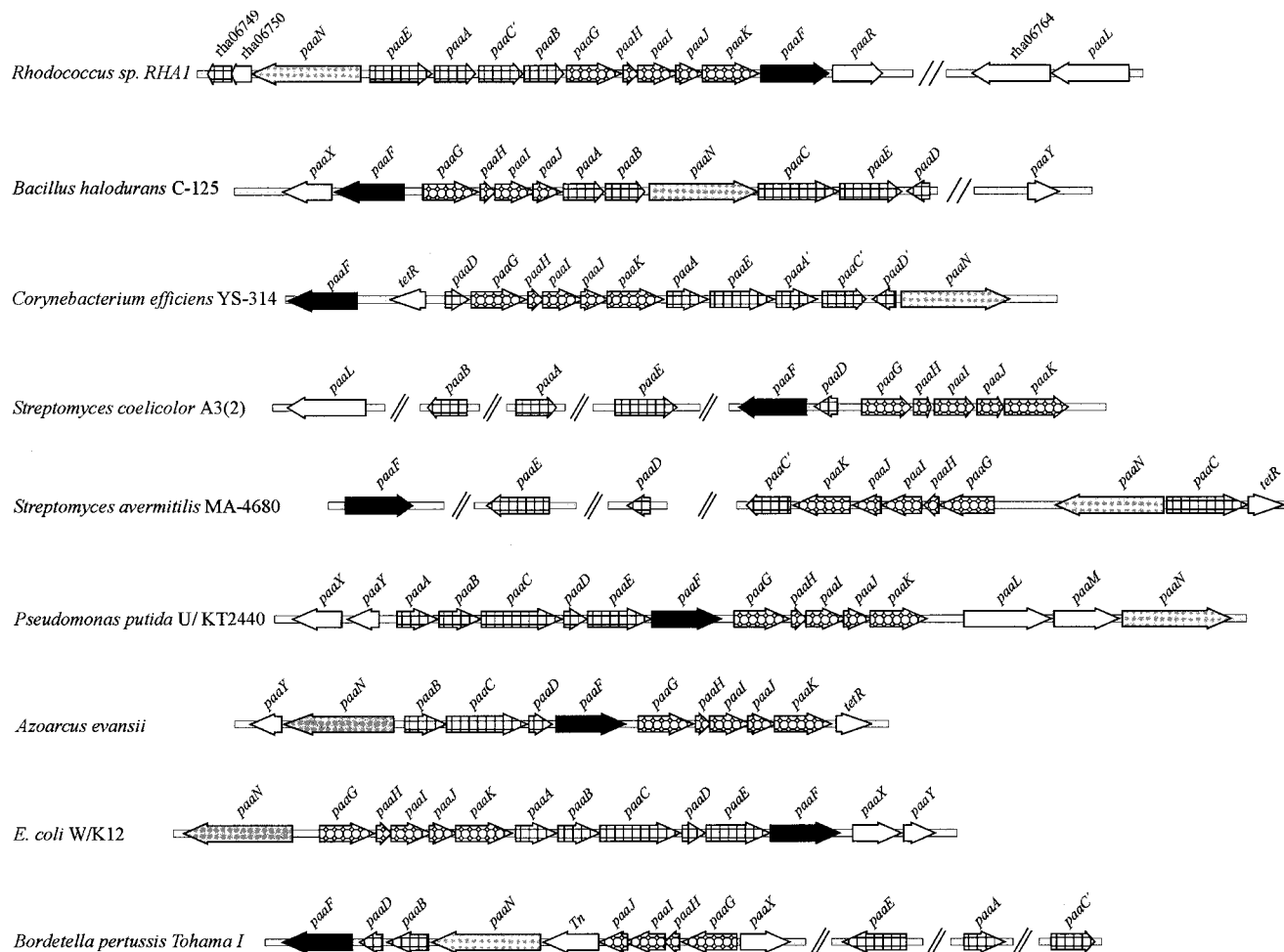


FIG. 4. Comparison of *paa* gene organizations in *Rhodococcus* sp. strain RHA1 and other bacteria. The gene names are in accordance with those listed in reference 12. Tn, transposase; TetR, TetR family regulator; *paaR*, an AraC-type regulator. Variants of *paa* genes are indicated with a prime (e.g., C', A', and D'). All sequences, except that of RHA1, were obtained from The Institute for Genomic Research (<http://www.tigr.org/tdb>) or NCBI (<http://www.ncbi.nlm.nih.gov>).

most of the *paa* genes were transcribed in PAA-grown cells (Fig. 2). Second, eight of the predicted Paa proteins were expressed in PAA-grown cells while being nondetectable in pyruvate-grown controls (Fig. 3; Table 2). Third, the *paaN* gene of RHA1 was essential for growth on PAA, as was previously reported for two gram-negative bacteria (8, 17). Fourth, the *paaN* mutant produced metabolites consistent with the predicted role of PaaN in the PAA pathway (Fig. 1). In agreement with our results, a *paaN* mutant of *Azoarcus evansii* was previously reported to accumulate tropone (17), and *paaN* mutants of *E. coli* were previously reported to accumulate 2-hydroxyphenylacetate (5, 8). While we did not detect the latter metabolite, we hypothesize that the 2-coumaranone we detected was formed from 2-hydroxyphenylacetate and that the methyl ester of 2-methoxyphenylacetate we detected was formed by derivatization of 2-coumaranone. Thus, the metabolites found in this study are all potential derivatives of the expected substrate for PaaN. The phenotype of the *paaN* mutant indicates that RHA1 does not have an alternative pathway for PAA catabolism or an alternative mechanism for transformation of phenylacetyl-CoA.

Although the *paaF* mutant of RHA1 was able to grow on PAA, its phenotype is consistent with involvement of PaaF in the PAA pathway. Unlike WT RHA1, the *paaF* mutant failed to completely remove PAA from the medium while growing on pyruvate. It appears that RHA1 possesses one or more CoA ligases that can partially complement PaaF. This possibility is supported by the existence of at least nine paralogs of *paaF* in the RHA1 genome, as well as over 50 other genes whose putative products show some sequence identity to known CoA ligases. The phenotype of the *paaF* mutant (Table 3) suggests that CoA ligases other than PaaF cannot transform 2-phenylethylamine and are limited in the transformation of phenylacetaldehyde and 2-phenylethanol. In contrast to RHA1, *P. putida* U (15) and *E. coli* (8) both require PaaF for growth on phenylacetate.

The organization of the *paa* genes differs among different organisms, but some features are common to all described *paa* clusters (Fig. 4). Genes encoding two core functional units of the pathway that are consistently clustered include *paaGHIJK* (encoding a ring-hydroxylating system) and, usually, *paaABCE*

(encoding a β -oxidation system). Other genes commonly occurring in *paa* gene clusters include *paaN* (encoding a putative ring-opening enzyme) and *paaF* (encoding an acetyl-CoA ligase). Apart from these genes, some *paa* gene clusters also contain genes encoding a transport system (e.g., *paaLM*) and genes encoding a regulatory system (e.g., *paaXY*) (5, 12, 15). Most of the components described above were found in a single gene cluster in *Rhodococcus* sp. strain RHA1. This clustering is in contrast to the gene organization of at least two other actinomycetes, *Streptomyces avermitilis* and *Streptomyces coelicolor*, in which there are homologs of several *paa* genes but in which only those encoding the ring-hydroxylating system, *paaGHIJK*, are clustered.

The *paaC* gene of RHA1 putatively encodes a 284-amino acid (aa) dehydrogenase similar to those in *S. avermitilis*, *Corynebacterium efficiens*, and *Bordetella pertussis* (Fig. 4). Homologs of these PaaC proteins are found in other gram-positive and gram-negative bacteria but are distinct in that they encode larger proteins (ca. 500 aa). A paralog of PaaC, encoded by rha07533, was detected only during growth on PAA (spot 9 in Fig. 3 and Table 2).

Associated with the *paa* gene cluster of RHA1 but independently transcribed is *paaL* (Fig. 2), which encodes a putative permease having ca. 40% aa identity with PAA permeases in *Pseudomonas putida* (AAC24338), *Pseudomonas* sp. strain Y2 (CAE45115, CAE45115, and CAD76939), and *Chromobacterium violaceum* (AAQ58580). For comparative purposes, it is difficult to identify phenylacetate transport systems in relatives of RHA1, such as *S. avermitilis* and *S. coelicolor*, because they lack clustered *paa* genes. In RHA1, there is no *paaM* gene adjacent to *paaL* or elsewhere, but this is not surprising since a porin encoded by *paaM* is presumably unnecessary in a gram-positive organism, which lacks an outer cell membrane.

In some genomes (*E. coli*, *Klebsiella pneumoniae*, and *Bacillus halodurans*), a *paa* regulator gene is downstream of *paaF* (12). Downstream of *paaF* in RHA1 is *paaR* (Fig. 4), whose product has the highest similarity to an AraC-type transcriptional regulator (Table 1) (10). The product of *paaR* may serve the function of the regulatory system encoded by *paaXY* in some gram-negative bacteria. Other actinomycetes, such as *S. coelicolor*, *S. avermitilis*, and *Corynebacterium efficiens*, also lack homologs of *paaXY* associated with *paa* genes, but the last two have genes encoding TetR-type regulators, which are negative regulators associated with *paa* genes. Our results (Table 3; Fig. 2 and 3) neither confirm nor contradict the possibility of a role for PaaR in regulating the *paa* genes. If PaaR does regulate *paa* gene expression, the phenotype of the *paaR* mutant suggests that it is likely a negative regulator.

It was recently suggested that the PAA degradation pathway is widely distributed and that *paa* genes may have horizontally transferred across bacterial phyla (1). The average GC content of the RHA1 *paa* gene cluster is the same as that of the RHA1 genome, and there are no transposase genes or other evidence of horizontal gene transfer in regions flanking the *paa* gene cluster of RHA1. Thus, despite the similarity of the Paa proteins to those in organisms with lower GC content, there is no evidence that the *paa* genes were recently obtained by RHA1 from another organism.

Seven substrates, including PAA, were determined to be part of the phenylacetyl-CoA catabolon of RHA1. These seven

substrates did not support growth of the *paaN* mutant (Table 3). Predictably, six substrates that were not expected to be degraded via the PAA pathway—pyruvate, benzene, biphenyl, mandelate, benzoate, and phthalate—supported very similar growth levels of RHA1 and the mutant strains. However, the *paaN* mutant also grew on styrene, ethylbenzene, and 3-hydroxyphenylacetate, despite the fact that these compounds are degraded via the PAA pathway in certain gram-negative bacteria (12, 17). It is likely that RHA1 degrades ethylbenzene via a pathway also used for biphenyl degradation (unpublished data). RHA1 might degrade styrene via 3-vinylcatechol, as has been proposed for *Rhodococcus rhodochrous* NCIMB 13259 (14, 21). Our results suggest that the phenylacetyl-CoA catabolon in RHA1 may be more limited than those of other organisms. However, the evidence does not exclude the possibility that the PAA pathway is partially responsible for the degradation of styrene, ethylbenzene, and 3-hydroxyphenylacetate (i.e., that different pathways might act simultaneously).

ACKNOWLEDGMENTS

We thank Manisha Dosanjh for developing the mutagenesis method and Christine Florizone for assistance with proteomic analyses.

This work was supported by a Genome Canada/Genome BC grant and by the Universidad Complutense Madrid (UCM) project PR1/03-11648. J.M.N.-L. was a recipient of a UCM-Flores Valles scholarship.

REFERENCES

1. Abe-Yoshizumi, R., U. Kamei, A. Yamada, M. Kimura, and S. Ichihara. 2004. The evolution of the phenylacetic acid degradation pathway in bacteria. *Biosci. Biotechnol. Biochem.* **68**:746–748.
2. Alvarez, H. M., H. Luftmann, R. A. Silva, A. C. Cesari, A. Viale, M. Wältermann, and A. Steinbüchel. 2002. Identification of phenyldecanoic acid as a constituent of triacylglycerols and wax ester produced by *Rhodococcus opacus* PD630. *Microbiology* **148**:1407–1412.
3. Datsenko, K. A., and B. L. Wanner. 2000. One-step inactivation of chromosomal genes in *Escherichia coli* K-12 using PCR products. *Proc. Natl. Acad. Sci. USA* **97**:6640–6645.
4. Denef, V. J., J. Park, T. V. Tsoi, J.-M. Rouillard, H. Zhang, J. A. Wibbenmeyer, W. Verstraete, E. Gulari, S. A. Hashsham, and J. M. Tiedje. 2004. Biphenyl and benzoate metabolism in a genomic context: outlining genome-wide metabolic networks in *Burkholderia xenovorans* LB400. *Appl. Environ. Microbiol.* **70**:4961–4970.
5. Ferrández, A., B. Miñambres, B. García, E. R. Olivera, J. M. Luengo, J. L. García, and E. Díaz. 1998. Catabolism of phenylacetic acid in *Escherichia coli*: characterization of a new aerobic hybrid pathway. *J. Biol. Chem.* **273**:25974–25986.
6. Flamm, R. K., D. J. Hinrichs, and M. F. Thomashow. 1984. Introduction of pAM β 1 into *Listeria monocytogenes* by conjugation and homology between native *L. monocytogenes* plasmids. *Infect. Immun.* **44**:157–161.
7. Gust, B., G. L. Challis, K. Fowler, T. Kieser, and K. F. Chater. 2003. PCR-targeted *Streptomyces* gene replacement identifies a protein domain needed for biosynthesis of the sesquiterpene soil odor geosmin. *Proc. Natl. Acad. Sci. USA* **100**:1541–1546.
8. Ismail, W., M. El-Said Mohamed, B. L. Wanner, K. A. Datsenko, W. Eisenreich, F. Rohdich, A. Bacher, and G. Fuchs. 2003. Functional genomics by NMR spectroscopy: phenylacetate catabolism in *Escherichia coli*. *Eur. J. Biochem.* **270**:3047–3054.
9. Kitagawa, W., A. Suzuki, T. Hoaki, E. Masai, and M. Fukuda. 2001. Multiplicity of aromatic ring hydroxylation dioxygenase genes in a strong PCB degrader, *Rhodococcus* sp. strain RHA1 demonstrated by denaturing gradient gel electrophoresis. *Biosci. Biotechnol. Biochem.* **65**:1907–1911.
10. Komeda, H., Y. Hori, M. Kobayashi, and S. Shimizu. 1996. Transcriptional regulation of the *Rhodococcus rhodochrous* J1 *nitA* gene encoding a nitrilase. *Proc. Natl. Acad. Sci. USA* **93**:10572–10577.
11. Kulakov, L. A., and M. J. Larkin. 2002. Genetic organization of *Rhodococcus*, p. 15–46. In A. Danchin (ed.), *Genomics of GC-rich gram-positive bacteria*. Caister Academic Press, Wymondham, United Kingdom.
12. Luengo, J. M., J. L. García, and E. R. Olivera. 2001. The phenylacetyl-CoA catabolon: a complex catabolic unit with broad biotechnological applications. *Mol. Microbiol.* **39**:1434–1442.
13. Masai, E., A. Yamada, J. M. Healy, T. Hatta, K. Kimbara, M. Fukuda, and K. Yano. 1995. Characterization of biphenyl catabolic genes of gram-positive polychlorinated biphenyl degrader *Rhodococcus* sp. strain RHA1. *Appl. Environ. Microbiol.* **61**:2079–2085.

14. O'Leary, N. D., K. E. O'Connor, and A. D. Dobson. 2002. Biochemistry, genetics and physiology of microbial styrene degradation. *FEMS Microbiol. Rev.* **26**:403–417.
15. Olivera, E. R., B. Miñambres, B. Garcia, C. Muñiz, M. A. Moreno, A. Fernández, E. Díaz, J. L. García, and J. M. Luengo. 1998. Molecular characterization of the phenylacetic acid catabolic pathway in *Pseudomonas putida* U: the phenylacetyl-CoA catabolon. *Proc. Natl. Acad. Sci. USA* **95**:6419–6424.
16. Patrauchan, M. A., C. Florizone, M. Dosanjh, W. W. Mohn, J. Davies, and L. D. Eltis. 2005. Catabolism of benzoate and phthalate in *Rhodococcus* strain RHA1: redundancies and convergence. *J. Bacteriol.* **187**:4050–4063.
17. Rost, R., S. Haas, E. Hammer, H. Herrmann, and G. Burchardt. 2002. Molecular analysis of aerobic phenylacetate degradation in *Azoarcus evansii*. *Mol. Genet. Genomics* **267**:656–663.
18. Sambrook, J., E. F. Fritsch, and T. Maniatis. 1989. *Molecular cloning: a laboratory manual*, 2nd ed. Cold Spring Harbor Laboratory Press, Cold Spring Harbor, N.Y.
19. Seto, M., E. Masai, M. Ida, T. Hatta, K. Kimbara, M. Fukuda, and K. Yano. 1995. Multiple polychlorinated biphenyl transformation systems in the gram-positive bacterium *Rhodococcus* sp. strain RHA1. *Appl. Environ. Microbiol.* **61**:4510–4513.
20. van der Geize, R., and L. Dijkhuizen. 2004. Harnessing the catabolic diversity of rhodococci for environmental and biotechnological applications. *Curr. Opin. Microbiol.* **7**:255–261.
21. Warhurst, A. M., K. F. Clarke, R. A. Hill, R. A. Holt, and C. A. Fewson. 1994. Metabolism of styrene by *Rhodococcus rhodochrous* NCIMB 13259. *Appl. Environ. Microbiol.* **60**:1137–1145.
22. Warren, R., W. W. L. Hsiao, H. Kudo, M. Myhre, M. Dosanjh, A. Petrescu, H. Kobayashi, S. Shimizu, K. Miyauchi, E. Masai, G. Yang, J. M. Stott, J. E. Schein, H. Shin, J. Khattra, D. Smailus, Y. S. Butterfield, A. Siddiqui, R. Holt, M. A. Marra, S. J. M. Jones, W. W. Mohn, F. S. L. Brinkman, M. Fukuda, J. Davies, and L. D. Eltis. 2004. Functional characterization of a catabolic plasmid from polychlorinated-biphenyl-degrading *Rhodococcus* sp. strain RHA1. *J. Bacteriol.* **186**:7783–7795.
23. Zaar, A., J. Gescher, W. Eisenreich, A. Bacher, and G. Fuchs. 2004. New enzymes involved in aerobic benzoate metabolism in *Azoarcus evansii*. *Mol. Microbiol.* **54**:223–238.